Journal of Advanced Research 24 (2020) 545–555

Contents lists available at ScienceDirect

Journal of Advanced Research

journal homepage: www.elsevier.com/locate/jare

Molecular networking aided metabolomic profiling of beet leaves using three extraction solvents and in relation to its anti-obesity effects

Nesrine M. Hegazi [a,*], Rasha A. Radwan [b], Sherein M. Bakry [a], Hamada H. Saad [a,c]

[a] Phytochemistry and Plant Systematics Department, Division of Pharmaceutical Industries, National Research Centre, PO Box 12622, Cairo, Egypt
[b] Biochemistry Department, Faculty of Pharmacy, Sinai University-Kantara Branch, El Ismailia, 41611, Egypt
[c] Department of Pharmaceutical Biology, Pharmaceutical Institute, Eberhard Karls University of Tübingen, PO Box 72074, Tübingen, Germany

GRAPHICAL ABSTRACT

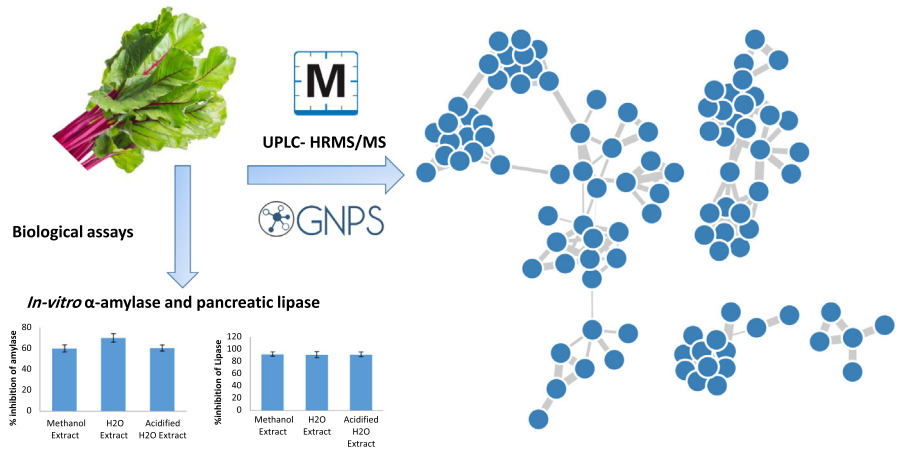

ARTICLE INFO

Article history:
Received 12 May 2020
Accepted 1 June 2020
Available online 3 June 2020

Keywords:
Beta vulgaris
UPLC-HRMS-MS
Molecular networking
α- amylase
Pancreatic lipase

ABSTRACT

In the present study, the efficiency of three different solvents (H_2O, acidified H_2O, and 70% Methanol) for metabolites extraction from the leaves of sugar beet (*Beta vulgaris* subsp. *vulgaris* var. *rubra*) was investigated along with their inhibitory activity on pancreatic α-amylase and lipase for obesity management. The metabolic profile of the three extracts was analyzed by ultra-performance liquid chromatography (UPLC) coupled with electrospray ionization high-resolution mass spectrometric (ESI-HRMS-MS). Mass spectrometry-based molecular networking was employed to aid in metabolites annotation and for the visual investigation of the known metabolites and their analogues. The study led to the tentative identification of 45 metabolites including amino acids, purine derivatives, phenolic acids, flavonoids, fatty acids, and an alkaloid, articulating 24 compounds as a first time report from beet leaves along with 2 new putatively identified compounds: a flavone feruloyl conjugate (**39**) and a malonylated acacetin diglycoside (**40**). The three extracting systems exhibited comparable efficiency for pulling out the secondary metabolites from the beet leaves. The *in vitro* study supported this finding and demonstrated that the three extracts inhibited the activity of both pancreatic α-amylase and lipase enzymes with no significant

Peer review under responsibility of Cairo University.
* Corresponding author at: Phytochemistry and Plant Systematics Department, National Research Centre, Dokki, Cairo, Egypt.
E-mail address: nm.hegazi@nrc.sci.eg (N.M. Hegazi).

https://doi.org/10.1016/j.jare.2020.06.001
2090-1232/

difference observed regarding the percentage of the inhibition of the enzymes. Conclusively, the extraction protocol has a minimal effect on the anti-obesity properties of beet leaves.

Introduction

Obesity is a growing universal issue and regarded as one of the utmost intimidations to global health in this era [1]. Statistically, more than two billion adults worldwide are overweight among which 650 million of them are clinically obese [2]. Currently, there are two distinct classes of drugs for obesity management [3]. The first class acts by the inhibition of pancreatic lipase (orlistat), and hence reducing intestinal fat absorption [4]. The second one counts on suppressing the appetiteor anorectics represented by sibutramine [5]. However, both medications have several drawbacks such as hypertension, xerostomia, decreased bowel movements, headache, and sleeplessness [6–8]. Accordingly, there is always a persistent demand for an alternative approach to effective and safe obesity control [9]. Even though the widespread daily practice of consuming various dietary supplements for obesity surveillance, their effectiveness and safety are poorly investigated and have not yet persuasively proved in such context [1].

Digestive enzymes such as pancreatic α-amylase and lipase are known to be responsible for the oligosaccharides and triacylglycerols hydrolysis into simple molecules. Naturally occurring polyphenols are firmly ascertained to inhibit such digestive enzymes which can govern the food caloric content by reducing its absorption and prolonging the digestive process. By this means, a bodyweight reduction could be an achievable task and consequently yield significant health improvement [10].

A substantial number of reports has accentuated the nutritional value and health benefits of functional foods. Special attention was given to vegetables and fruits for their overall wellbeing effects including reduced incidence of metabolic, cardiovascular disorders, and cancers [11–13].

Beta vulgaris L. species belong to the Amaranthaceae family and is widely distributed throughout Asian Turkey, the Mediterranean, and Europe [14]. The species is recognized in traditional medicines as an immunostimulant and as adjuvant therapy in cancer treatment [15]. The Red beetroot '*Beta vulgaris*, subsp. *vulgaris* var. *rubra*' is widely used in folk medicines, besides its widespread use in the food industry as food colouring [16]. Red beets represent a rich source of natural nitrates which proved helpful in diseases associated with low bioavailability of NO including hypertension and endothelial function [17]. Several *in vivo* and *in vitro* reports demonstrated innumerable biological activities for beetroots including antioxidant and anti-inflammatory [18], antimicrobial [19], stimulant of the hematopoietic and immune systems; renal and hepatic protective, antioxidant, anti-inflammatory and antitumor properties [20]. The antioxidant and antidiabetic potential of beetroots advocates its possible use in obesity management [21,22].

Beetroot phytochemicals were previously extracted with various solvents including distilled water [23], 80% alcohol [24,25], and acidified ethanol with citric acid [26,27]. Nevertheless, significant differences were observed in the content of the individual compounds as affected by the solvent choice [25].

In this context and motivated by the public usage of beets and its documented biological properties, this study fundamentally focused on the exploration of the phytochemical constituents of three different extracts (aqueous, acidified aqueous with 1% ascorbic acid and 70% methanol) of *B. vulgaris* (sugar beet) leaves using UPLC-PDA-(±) ESI-HRMS/MS . Mass spectral similarity networking *via* the global natural products social molecular networking platform (GNPS) was employed for the visualization and exploration of the tandem mass spectrometry data and to aid in dereplication of known metabolites and their possible analogues. Simultaneously, the diminishing effect of the three extracts of *B. vulgaris* leaves on pancreatic α-amylase and lipase enzymes were inspected for their potential use for obesity management.

Materials and methods

Plant material

Sugar beet leaves (*Beta vulgaris*, subsp. *vulgaris* var. *rubra)* were obtained from local merchandise in Giza, Egypt in March 2018. A plant sample was verified by Prof. Dr. Salwa Khawatshi, professor of Taxonomy, National Research Centre, Cairo, Egypt. A voucher specimen (M132) was deposited in the herbarium of the National Research Centre (CAIRC), Phytochemistry and Plant Systematics Department, National Research Centre, Dokki, Cairo, Egypt. The leaves were cleaned thoroughly from the fine dust and debris with bi-distilled H_2O, ground to paste, and frozen at −20 °C for further analysis.

Chemicals

Methanol (HPLC grade) was obtained from Fisher Chemical, UK. Sodium formate (MS grade) was provided by Honeywell Fluka, Germany. All other chemicals for phytochemical analysis and biological assays were purchased from Sigma-Aldrich (Merck, USA).

Preparation of the extracts

To extract the beet leaves metabolites, three different solvents were used: bi-distilled H_2O (**a**), acidified bi-distilled H_2O with 1% (w:v) ascorbic acid (**b**) and 70:30 MeOH: bi-distilled H_2O (**c**). For each extracting solvent, 500 ml were used to sonicate 250 g of leaves for 30 min at 50 °C, each in triplicates. Extracts were then filtered, evaporated under reduced pressure, and finally lyophilized and kept frozen at −20 °C.

Sample preparation for HPLC profiling and MS analyses

The lyophilised samples of the three extracts (50 mg each) were dissolved in 70% MeOH (HPLC-grade) with sonication (10 mins), then centrifuged. Aliquots were then evaporated under reduced pressure followed by freeze-drying for 48 hrs. For HPLC profiling, 10 mg of the dried extracts were dissolved in 500 μl MeOH (HPLC-grade), each in triplicates, and 10 μl were injected. Meanwhile, triplicates of 1 mg in 250 μl MeOH (MS-grade) were prepared for MS analysis consuming 5 μl as an injection volume in the UPLC-MS analysis.

HPLC profiling

Profiling of the obtained extracts triplicates was achieved using an HPLC system composed of Waters 1525 Binary Pump with a 7725i Rheodyne injection port; a Kromega Solvent Degasser:

Waters 996 Photodiode Array Detector; and an Aeris peptide XB-C18 (5 μm, 250 × 4.6 mm, Phenomenx). ACN (solvent A) and H_2O + 0.1% TFA (solvent B) were used for the gradient elution of the analytes at a steady flow rate of 0.7 ml/min, with an injection volume of 5 μl. A non-uniform gradient was employed: for the initial 8 min, 10% A, then 30% A for 12 min, 35% A for additional 15 min, 50% A for 10 min, followed by 100% A for 10 min, 20% A for 1 min, and lastly 10% A for the last 4 min. The detection wavelengths were 238, 280, and 336 nm.

UPLC-HRMS-MS analysis

MaXis-4G instrument (Bruker Daltonics, Bremen, Germany) attached to an Ultimate 3000 HPLC (Thermo Fisher Scientific) were used for HR-MS analysis. The HPLC-method was (0.1% FA in H_2O as solvent A and MeOH as solvent B), an isocratic gradient of 10% B for 10 min, 10% to 100% B in 30 min, 100% B for an additional 15 min, using a flow rate of 0.3 ml/min; 5 μl injection volume and UV detector (UV/VIS) wavelength monitoring at 336, 280 and 238 nm. The separation was performed on a Nucleoshell 2.7 μm 150 × 2 mm column (Macherey-Nagel), and the range for MS acquisition was *m/z* 50–1800. A capillary voltage of 4500 V, nebulizer gas pressure (nitrogen) of 2 (1.6) bar, ion source temperature of 200 °C, the dry gas flow of 9 L/min source temperature, and spectral rates of 3 Hz for MS^1 and 10 Hz for MS^2 were used. For MS/MS fragmentation, the 10 most intense ions per MS^1 were chosen for subsequent CID with stepped CID energy applied. The employed parameters for tandem MS were applied following [28]. Sodium formate was used as a calibrant, and with acquired data calibrated using a Bruker-developed script.

Data analysis and preprocessing

Data visualization was performed using Bruker Daltonics Data Analysis 4.4, while Metaboscape 3.0 (Bruker Daltonics) was used for molecular features selection. Raw data files were imported into MetaboScape 3.0 for the entire data treatment and pre-processing. T-ReX 3D (Time aligned Region Complete eXtraction) algorithm was used for retention time alignment. It automatically detects and combines isotopes, adducts, and fragments intrinsic to the same compound into one feature. All detected features were displayed as a bucket table with their Rt, measured *m/z*, molecular weight, detected ions, and their intensity in each sample [29]. The Bucket table was created with intensity threshold $10e^3$ and $10e^4$ for negative and positive ionization modes, respectively. The retention time range was set from 1 to 35 min and the mass range from 140 to 1800 *m/z*.

Molecular networking and metabolites annotation

The features list of the three extraction solvents was exported from Metaboscape as two single MGF files for both of the positive and negative measurements. Both MGF files were uploaded separately to the GNPS online platform where two molecular networks were generated with the online workflow (GNPS 2.0). A molecular network was created with a cosine score above 0.65 and 0.7 for positive and negative modes, respectively. The minimum number of matched fragment ions was adjusted to 6. Further edges between two nodes were kept in the network if (and only if) each of the nodes appeared in each other's respective top 10 most similar nodes. The network spectra were searched against GNPS' spectral libraries using a minimum of 6 matched fragments for spectral matching. Cytoscape 3.5.1 was used for molecular network visualization.

Manual putative structures identification was achieved by submitting the preprocessed MS^2.mgf output file from Metaboscape to Sirius + CSI: FingerID 4.0.1 for the prediction of elemental composition (C, H, N, O, S, P) and molecular structure database search with *m/z* tolerance set to 20 ppm using online Pubchem database [30,31] and DEREP-NP database which was manually integrated into the software [32].

Alpha-amylase inhibition

The α-amylase bioassay was performed as described by Miller with some modifications [33,34]. In brief, potato starch was mixed with 20 mmol L^{-1} sodium phosphate buffer with 6.7 mmol L^{-1} sodium chloride to obtain a 0.5% w/v starch solution. For the preparation of the enzyme solution, 25.3 mg of α-amylase (10 U mg^{-1}) was stirred in 100 ml of cold distilled water. Extracts solutions were made by dissolving them in a buffer to afford a final concentration ranging from 1000 μg mL^{-1} to 31.25 μg mL^{-1}. Sodium potassium tartrate solution (12.0 g of sodium potassium tartrate tetrahydrate in 8.0 ml of 2 M NaOH) and 96 mmol L^{-1} of 3, 5 dinitro salicylic acid solution were mixed for the colourimetric reagent. The control (acarbose as a positive control) and the extracts solutions with concentrations (75–600 μg/mL) were mixed individually with the starch solution and allowed to react with α-amylase in alkaline conditions at 25°C. Maltose production was quantified by the reduction of 3,5-dinitrosalicylic acid to 3-amino5-nitrosalicylic acid. The reaction was detected at 540 nm using ELX 808 (Bio-Tek Instrumental, Italy). The following equation was employed for the calculation of the percentages of inhibition: 100- [{A sample/ A control × 100].

Pancreatic lipase inhibition

Following Conforti protocol [35], the inhibition of pancreatic lipase was evaluated. Pancreatic lipase aqueous solution (1 $mgmL^{-1}$) was made from type II crude porcine enzyme. The solution of 4-nitrophenyl octanoate (NPC) (5 mmol L^{-1}) in dimethyl sulfoxide was prepared as the substrate. The reaction mixture was executed as follows: 100 μl of 5 mmol L^{-1} NPC, 4 ml of Tris-HCl buffer (pH = 8.5), 100 μl of extract solutions in concentrations from (12–100 μg/ mL), and 100 μl of enzyme solution. Next, the prepared solution was incubated at 37 °C for 25 min before adding the substrate. For the negative control, the same volume of dimethyl sulfoxide was added instead of the extract solution. The absorbance was measured in cuvettes at 412 nm using ELX 808 (Bio-Tek Instrumental, Italy). A blank sample without the enzyme was measured for each extract. For comparison, orlistat was used as a positive control at a final concentration of 20 μgmL^{-1}.The following formula was used to calculate the percentage of inhibition: 100- [{A sample/ A control} × 100].

Statistical analysis

Both enzymatic experiments were carried out in triplicates. The results were given as mean values and standard deviations (SDs). The differences among the various extracts were analyzed using a one-way analysis of variance (ANOVA) followed by Tukey's honest significant difference post hoc test at p values < 0.05 [36]. A linear regression curve was employed to calculate the IC_{50} (extract concentration that inhibits 50% of the enzyme activity). The horizontal axis displayed the concentrations of the extracts, which were (from 75 to 600 μg/ml) for α-amylase and (from 60 to 600 μg/ml) and pancreatic lipase. While the vertical axis presented the percentage of inhibition [37]. All analyses were calculated using SPSS v. 22.0 (IBM, Chicago, USA). Microsoft Excel 2010 was used for graph construction.

Results and discussion

HPLC and UPLC-HRMS/MS metabolites profiling of the extraction solvents

This study aimed to chart the comparable efficiency of three different extracting solvents in terms of as many as attainable metabolites from beet leaves. The HPLC profiling of the three different extracts including the triplicates exhibited insignificant differences as seen in **Suppl. Fig. S1** suggesting that the three solvent (s) mixtures could be similarly and efficiently used for extracting the beet leaves metabolites under the studied conditions.

Driven by the high similarity in the HPLC readings of the different extracts, a holistic comparative secondary metabolic analysis of the red beet leaves for 3 different extraction solvents was necessitated *via* reversed-phase (RP-C18) UPLC-PDA-ESI-HRMS/MS in both ionization modes. Overlaid base peak chromatogram (BPC) for the three solvents is shown in Fig. 1.

Molecular networking-based categorization of beet leaves metabolites

Molecular networking depends on the fact that structurally similar metabolites have similar MS/MS fragmentation patterns allowing for the instantaneous visual investigation of identical molecules, analogues, or compound families [38]. In other words, it groups mass spectrometric data by mining spectral similarity between the MS/MS fragmentation patterns of different but structurally related metabolites. Within the network, each node corresponds to one consensus MS/MS spectrum, and is typically labeled with the neutral precursor mass. Nodes having common fragmentation patterns are connected with edges (lines). In this study, node and edge attributes were used, so that the colour of the node corresponds to the origin of the sample (used extraction solvent). Nodes were displayed as a pie chart to reflect the semi-relative abundance of each ion in the three extracts. The edges were employed using either their thickness as a caliber to the similarity between the connected nodes or as a measure of the mass shifts between the associated variants during the dereplication process.

Two networks were separately generated for the positive and negative ionization modes using the GNPS 2 platform (Figs. 2 & 3). The positive network contained 107 nodes compromising 8 clusters and 71 self-looped nodes whereas the negative afforded a total of 88 nodes arranged into 10 clusters and 49 self-looped nodes. The created networks allowed the visual inspection of the different compound families, analogues and aided in isomers discrimination. Clusters **A** in positive network, **A** & **B** in the negative network comprised the *C*-glycosidic flavones and their acylated derivatives (Figs. 2 & 3). Nevertheless, cluster **A** (Fig. 3) in the positive network was the one mostly used for the exploration of *C*-glycosidic flavones complemented with their fragmentation pattern in the negative ionization mode. While in the negative network (Fig. 2), clusters **C**, **D,** and **E** represented the flavonol *O*-glycosides, phenolic acids, and fatty acids, respectively. Other identified metabolites appeared as self-looped nodes within both of the networks.

UPLC-HRMS/MS metabolites annotation

Putative metabolites annotation was counted based on their retention times, molecular formula, UV absorption maxima, and their fragmentation pattern in comparison to previously reported data aided with the molecular networking investigation and GNPS

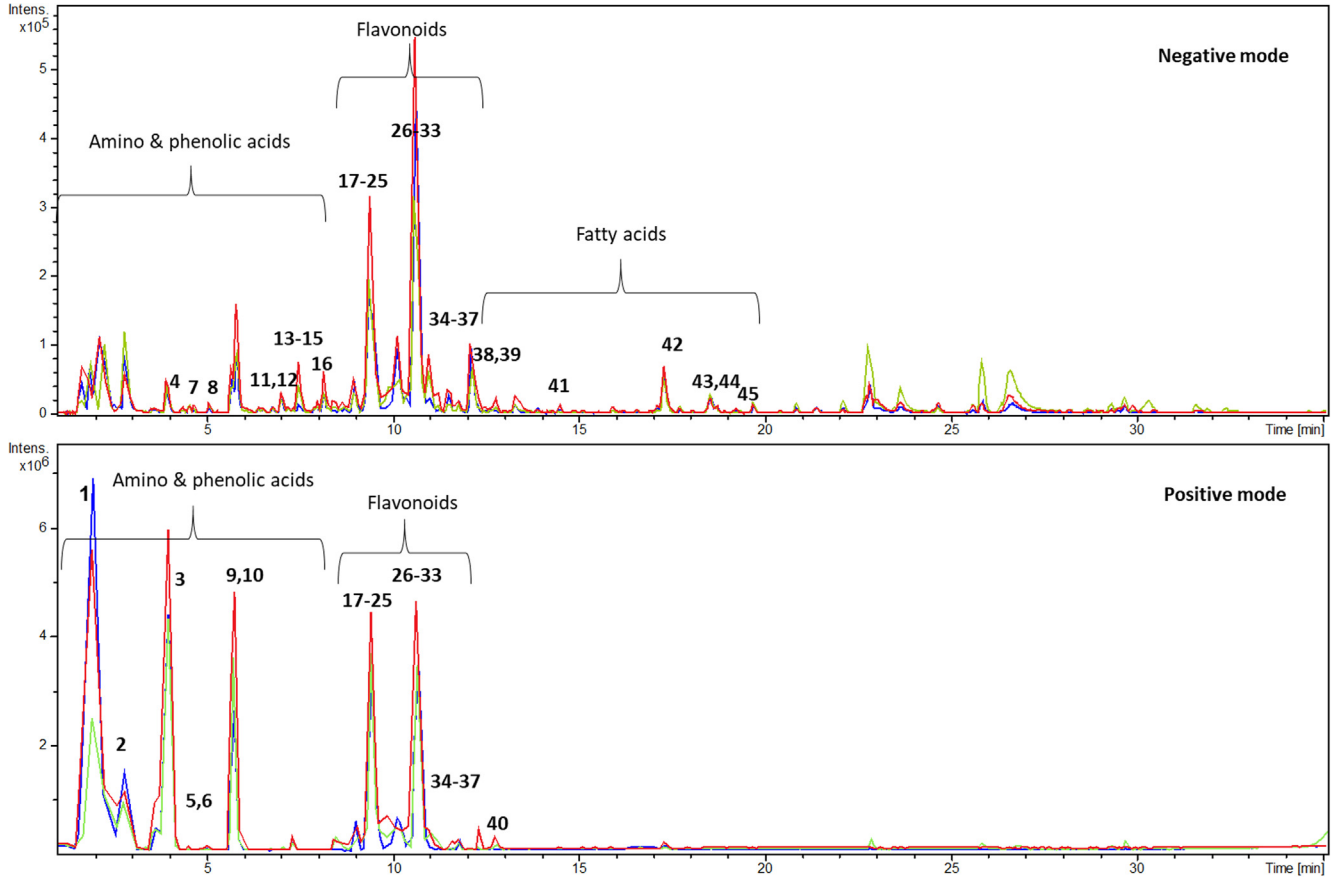

Fig. 1. Overlaid base peak chromatograms of the three extracts of beet leaves in the negative & positive ionization modes. Red colour: H_2O extract, green: acidified H_2O extract and blue 70% MeOH extract.

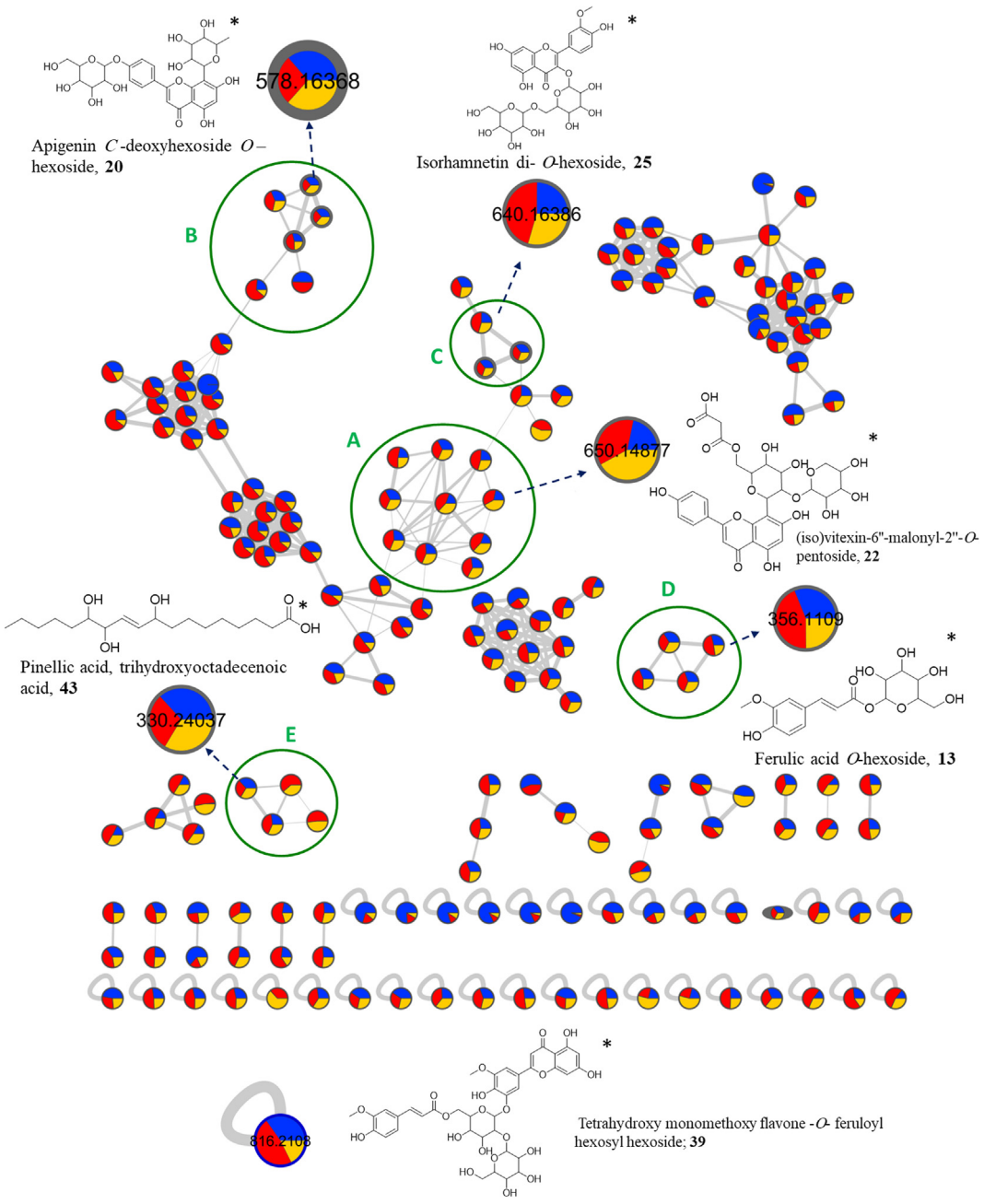

Fig. 2. Full molecular networking created using MS/MS data in negative mode from extracts of the leaves of *B. vulgaris* subsp. *vulgaris* var *rubra*. Nodes are labelled with parent mass. The network is displayed as pie chart with blue, red and orange colours representing distribution of theprecursor ion intensity in the acidified H_2O, H_2O, 70% MeOH extracts correspondingly. While, nodes with bold edges are nodes which matched with GNPS spectral libraries. * Substitution may differ.

spectral library search combined with the suggested fragmentation trees by Sirius. In total, 45 compounds belonging to different metabolite classes were tentatively identified including amino acids, purine derivatives, phenolic acids, flavonoids, fatty acids, and an alkaloid (Table 1). More than 50% of the annotated features (24 compounds, chiefly phenolic acids, and *C*-glycosidic flavones) are reported for the first time from the beet leaves along with 2 new putatively identified metabolites as a flavone feruloyl conjugate (**39**) and malonylated acacetin glycoside (**40**).

Amino acids and derivatives: Glutamine **1** and tryptophan **9** [39] were detected only in the positive mode whilst tryptophan *N*-glycoside **8** [40] was observed in the negative mode and appeared in the spectral network as self-looped nodes. Their identifications were based on their retention times, UV absorbance, molecular formula, and their fragmentation patterns.

Purine derivatives: Guanosine **2** and methylbutenyl isoguanine **5** were also annotated as stated earlier [41,42].

Alkaloids: A self-looped node in the positive spectral network was found for the first time abundantly in the H_2O extract of beet leaves as a pyrrolizidine alkaloid, trachelanthine **6**. It exhibited a molecular ion at *m*/*z* 302.1956 $[M + H]^+$ with a formula of $C_{15}H_{27}NO_5$ and a characteristic product ion at *m*/*z* 184.17 $[M + H\text{-}C_6H_{14}O_2]$ in accordance with Hama & Strobel, 2019 [43].

Phenolic acids and their derivatives:

The negative network using MS/MS data managed to gather the closely related phenolic acid glycosides together as cluster **D** encompassing compounds **4, 7**, **13,** and **14** (Fig. 2). Dihydroxy benzoic acid methyl ester-*O*-hexoside, **4** had a parent ion at *m*/*z*

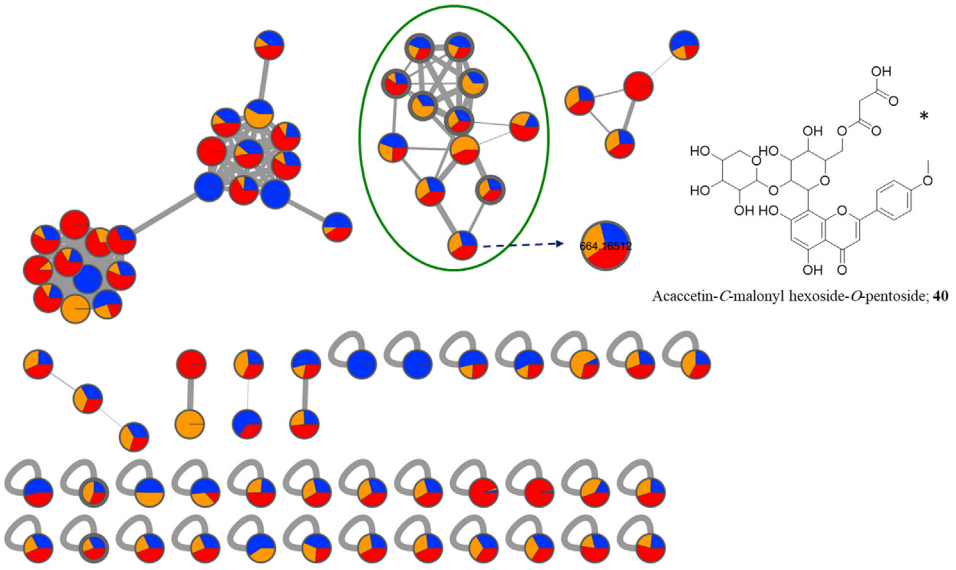

Fig. 3. Full molecular networking created using MS/MS data in the positive mode from extracts of the leaves of *B. vulgaris* subsp. *vulgaris* var *rubra*. Nodes are labelled with parent mass. The network is displayed as pie chart with blue, red and orange colours representing distribution of theprecursor ion intensity in the acidified H_2O, H_2O, 70% MeOH extracts correspondingly. While, nodes with bold edges are nodes which matched with GNPS spectral libraries. * Substitution may differ.

329.087 $[M-H]^-$, $C_{14}H_{18}O_9$ and a base peak at 167 $[M-H-162]^-$, due to the loss of the hexose moiety [44]. Meanwhile, compound **7**, *m/z* 359.0986 $[M-H]^-$ as $C_{15}H_{20}O_{10}$, was connected to **4** with a mass difference of 30 Da as a possible extra OCH_2. The fragments observation at *m/z* 197 $[M-H-162]^-$ and *m/z* 153 $[(M-H-162)-44]^-$ referring to the elimination of hexose moiety and CO_2, respectively eased its assignment as syringic acid hexoside **7** [45]. Ferulic acid hexoside **13** and sinapic acid hexoside **14** were also allied in the same cluster exhibiting in their negative MS^2 distinctive fragment ions at *m/z* 193 and *m/z* 223 owing to identical losses of *O*-hexosyl moiety, respectively [22,46].

While other phenolic features **3** & **11** were marked as self-looped nodes in the negative network due to their different fragmentation behavior which was reflected in their putative identities either as a non– or di-glycosylated species in contrast to **4, 7**, **13** and **14** assumed to be mono-glycosylated variants. Thus, compound **3** was assigned to be 2-hydroxyl-cinnamaldehyde, with a molecular ion at *m/z* 149.0600 $[M + H]^+$, and a molecular formula $C_9H_8O_2$ with fragment ions formed by losses of H_2O (-18 Da) and CO (-28 Da) [47]. However, Compound **11** was annotated as hydroxyl benzoyl hexosyl deoxyhexoside with *m/z* 445.1351$[M-H]^-$, $C_{19}H_{26}O_{12}$ supported by the characteristic product ions at *m/z* 283 $[M-H-162]^-$ for the loss of a hexose motif and *m/z* 137 $[M-H-162-146]^-$ for the consecutive loss of a deoxyhexoside moiety [48]. Assisted by spectral similarity networking, the occurrence of 2-hydroxyl-cinnamaldehyde **3**, dihydroxybenzoic acid methyl ester-*O*-hexoside **4**, syringic acid hexoside **7** and hydroxy benzoyl hexosyl deoxyhexoside **11** was possible for the first time in beet leaves.

Ferulic acid conjugates appeared as scattered four nodes in the negative network implying their peculiar fragmentation behavior. Compound **12** was assigned as feruloyl pentosyl-hexoside based on its molecular ion at *m/z* 487.1453 $[M-H]^-$, $C_{21}H_{28}O_{13}$ and its characteristic base peak at *m/z* 193 after losing pentosyl and hexosyl moieties [46]. Compound **15**, *m/z* 459.1506 $[M-H]^-$ with a formula of $C_{20}H_{28}O_{12}$ as non-previously reported feature in *B. vulgaris*, was dereplicated as butane-tetraol (*O*-feruloyl) -*O*- hexoside (paederol B) evidenced by a daughter ion at *m/z* 193 $[(M-H-162)-104]^-$ thanks to the losses of a hexose and butan-tetraol moieties [49]. Similarly, a parent ion $[M-H]^-$ at *m/z* 443.1199 with two key fragment ions at *m/z* 267 $[M-H-176]^-$ suggesting glucoronic acid moiety loss and *m/z* 193 $[M-H-176-73]^-$ for the glucoronosyl glycerol allowed the characterization of compound **16** as feruloyl glucuronosyl glycerol, formerly found in *B. vulgaris* cell cultures but not from beet leaves [50]. An additional *N*-containing phenylpropanoid was found to be a *N*-feruloyl-methoxytyramine **41** with a molecular formula of $C_{19}H_{21}NO_5$, *m/z* 342.1352 $[M-H]^-$, alongside two characteristic peaks at *m/z* 178, and 148 as previously described in the literature [51].

C- glycosidic flavones and their acylated derivatives:

Flavone *C*-glycosides were the most abundant metabolite class in the beet leaves. They compromised cluster **A** in the positive and **A** & **B** in the negative spectral networks (Figs. 2 & 3). MS/MS could nicely differentiate between *O*-glycosyl and *C*-glycosyl derivatives. Neutral losses of 162 / 132 or 146 corresponds to *O*-hexoside / pentoside or deoxyhexoside, respectively. Whereas, the fragmentation of *C*-glycosylated derivatives exhibits loss of H_2O [M-18], and cross ring cleavages of the sugar moieties observed as [M-120/90] $^{+/-}$ for *C*-hexosides, [M-90/60] $^{+/-}$ for *C*-pentosides and [M-104/47] $^{+/-}$ for *C*- deoxyhexosides [52]. Additionally, neutral losses of 42 and 86 accounts for acetylation and malonylation, respectively [46]. Further, the dereplication of the *C*- glycosidic flavones was much facilitated with the created networks that allowed the visualization of analogues and the quick discrimination of isomers, if any. The mass differences between the connected nodes accentuated the underlying structure modifications. For instances, mass differences of 14 Da or 30 Da were often due to a sugar replacement (pentoside to hexoside and *vice versa*), while 42 Da and 86 Da were characteristic of acetylated and malonylated descendants, respectively. While the acetylated and malonylated derivatives were connected together with 44 Da mass difference.

The first eluted flavone glycoside was (iso)vitexin 6''-*O*-pentoside **10**, which had a parent ion at *m/z* 565.1570 $[M + H]^+$, $C_{26}H_{28}O_{14}$ and an abundant ion at *m/z* 433 $[M + H-132]^+$ for the loss of a pentose unit and *m/z* 313 $[(M + H-132)-120]^+$ characteristic for the cross ring cleavage of *C*-glycosyl derivatives [52].

Table 1
Identified metabolites in the different extracts of the leaves of *B. vulgaris* subsp. *vulgaris* var. *rubra*.

Compound number	Rt (min)	Proposed structure	$[M + H]^+$	$[M-H]^-$	MS^2	Molecular formula (error in ppm)	Extraction solvent			References
							a	b	C	
1	1.76	Glutamine	175.1197		129	$C_6H_{14}N_4O_2$, (3.9)		√		[39]
2	2.85	Guanosine	284.0996		152	$C_{10}H_{13}N_5O_5$, (2.2)	√		√	GNPS libraries, [41]
3	4.1	Hydroxy-cinnamaldehyde*	149.0600		121, 130	$C_9H_8O_2$, (1.9)	√	√	√	[47]
4	4.13	Dihydroxybenzoic acid methyl ester-*O*-hexoside *		329.087	167, 152, 123	$C_{14}H_{18}O_9$, (0.92)	√	√	√	[44]
5	4.2	Methylbutenyl isoguanine*	220.1185		130	$C_{10}H_{13}N_5O_5$, (3.6)	√			[42]
6	4.57	Trachelanthine*	302.1956		184, 123	$C_{15}H_{27}NO_5$, (1.71)	√	√	√	[43]
7	4.6	Syringic acid *O*- hexoside*		359.0986	197, 153	$C_{15}H_{20}O_{10}$, (0.63)	√	√	√	[45]
8	5.03	Tryptophan *N*-hexoside		365.1356	203	$C_{17}H_{22}N_2O_7$, (1.59)	√		√	[40]
9	5.9	Tryptophan	205.0977		188, 146, 118	$C_{11}H_{12}N_2O_2$, (2.5)	√	√		GNPS libraries, [39]
10	5.8	6''-*O*-pentosyl (iso)vitexin	565.157		433, 313	$C_{26}H_{28}O_{14}$, (3.2)	√	√	√	GNPS libraries, [52]
11	6.11	Hydroxybenzoyl *O*-hexosyl-*O*-deoxyhexoside*		445.1351	283, 137	$C_{19}H_{26}O_{12}$, (0.32)	√	√	√	[48]
12	6.91	Ferulic acid *O*-pentosyl-hexoside		487.1453	193	$C_{21}H_{28}O_{13}$, (0.84)	√	√	√	[46]
13	7.04	Ferulic acid *O*-hexoside		355.1035	193, 178,	$C_{16}H_{20}O_9$, (0.2)	√	√	√	[22,46]
14	7.48	Sinapic acid -*O*- hexoside		385.1145	223, 208	$C_{17}H_{22}O_{10}$, (1.2)	√	√	√	[46]
15	7.63	Butane-tetraol-*O*-feruloyl-*O*-glucopyranoside. paederol B*		459.1506	193, 175	$C_{20}H_{28}O_{12}$, (0.13)	√	√	√	[49]
16	8.62	Ferulic acid-*O*-glucuronosyl glycerol		443.1199	267, 249, 193, 175, 134	$C_{19}H_{24}O_{12}$, (1.37)	√	√	√	[50]
17	9.04	Apigenin di- *C*-hexoside	595.1513	593.1515	473, 413, 313	$C_{27}H_{30}O_{15}$, (0.34)	√	√	√	[53]
18	9.12	Apigenin di- *C*-hexoside isomer	595.1595	593.1515	473, 413, 313	$C_{27}H_{30}O_{15}$, (1.77)	√	√	√	[53]
19	9.3	Apigenin -*C*- -deoxyhexoside *O* – hexoside*	579.1717	577.1567	415, 311	$C_{27}H_{30}O_{14}$, (0.72)	√	√	√	GNPS libraries, [52]
20	9.41	Apigenin *C* -deoxyhexoside *O* – hexoside isomer*	579.1702	577.1567	415, 311	$C_{27}H_{30}O_{14}$, (0.72)	√	√	√	GNPS libraries, [52]
21	9.48	2'' *O*-pentosyl (iso)vitexin		563.1410	413, 293	$C_{26}H_{28}O_{14}$, (0.6)	√	√	√	GNPS libraries, [54]
22	9.50	(iso)vitexin-6''-malonyl-2''-*O*- pentoside	651.1561	649.1403	563, 455, 311	$C_{29}H_{30}O_{17}$, (0.725)	√	√	√	[46]
23	9.6	Acetyl 2'' *O*-pentosyl (iso)vitexin*		605.1523	563, 413, 293	C28H30O15 (0.1)	√	√	√	[55]
24	9.92	Apigenin -*C*- hexoside	433.1136	431.1054	313, 283	$C_{21}H_{20}O_{10}$, (2.04)	√	√	√	[22]
25	9.99	Isorhamnetin di- *O*-hexoside	641.172	639.1565	317, 315	$C_{28}H_{32}O_{17}$, (1.35)	√	√	√	[46]
26	10.15	malonyl (iso)vitexin 2''-*O*-hexoside	681.1599	679.152	575, 455, 311, 293	$C_{30}H_{32}O_{18}$, (0.32)	√	√	√	[46]
27	10.23	Acetyl apigenin- *C*-pentoside- *C*-hexoside*		605.1521	563, 545, 455, 353, 311	$C_{28}H_{30}O_{15}$, (1.61)	√	√	√	[52]
28	10.25	(iso)vitexin 6''-acetyl 2''-*O*- hexoside*		635.1626	455, 413, 293	$C_{29}H_{32}O_{16}$ (0.2)	√	√	√	[52]
29	10.26	(iso)vitexin-6''-malonyl-2''-*O*- pentoside	651.1556	649.1415	563, 455, 311	$C_{29}H_{30}O_{17}$, (1.38)	√	√	√	[46]
30	10.39	Isorhamnetin -*O*- pentoside *O*-hexoside*		609.1465	315	$C_{27}H_{30}O_{16}$ (0.2)	√	√	√	GNPS libraries, [58]
31	10.45	Isorhamnetin -*O*- pentoside *O*- hexoside isomer*		609.1461	315	$C_{27}H_{30}O_{16}$ (0.2)	√	√	√	GNPS libraries, [58]
32	10.48	malonyl 6''-*O*-deoxyhexosyl -*C*-hexosyl apigenin *		663.1633	545, 311	$C_{30}H_{32}O_{17}$, (0.9)	√	√	√	[52]
33	10.62	Acetyl apigenin- *C*-pentoside- *C*-hexoside*		605.1515	563, 545, 455, 353, 311	$C_{28}H_{30}O_{15}$, (0.44)	√	√	√	[52]
34	11.02	Malonyl (iso)vitexin *	519.114	517.0986	413, 341, 311	$C_{24}H_{22}O_{13}$, (0.07)	√	√	√	[57]
35	11.2	Acacetin di- *C*-hexoside*		607.1669	487, 293	$C_{28}H_{32}O_{15}$ (2.1)	√	√	√	[56]
36	11.3	malonyl 6''-*O*-deoxyhexosyl -*C*-hexosyl apigenin *		663.1561	545, 311	$C_{30}H_{32}O_{17}$, (0.85)	√	√	√	[52]
37	11.8	Acacetin-*C*-hexoside −2''-*O*-pentoside*	579.1716	577.1565	427, 307	$C_{27}H_{30}O_{14}$, (1.9)	√	√	√	[39]
38	12.06	Dihydroxy dimethoxy flavone -*C*-hexoside 2''- *O* pentoside*		607.1636	457, 337	$C_{28}H_{32}O_{15}$ (2.3)	√	√	√	[52]
39	12.61	Tetrahydroxy monomethoxy flavone -*O*-feruloyl hexosyl hexoside**		815.2035	639, 315	$C_{38}H_{40}O_{20}$, (0.15)	√	√	√	
40	12.8	Acacetin-*C*-malonyl hexoside-*O*-pentoside**	665.1723		533, 447, 327	$C_{30}H_{32}O_{17}$, (1.75)	√		√	
41	14.27	*N* -feruloyl-methoxytyramine		342.1352	178, 327, 148	$C_{19}H_{21}NO_5$, (1.44)	√	√	√	[51]
42	17.3	Trihydroxy-octadecadienoic acid		327.2178	211	$C_{18}H_{32}O_5$, (0.4)	√		√	[59]

(*continued on next page*)

Table 1 (*continued*)

Compound number	Rt (min)	Proposed structure	[M + H]$^+$	[M−H]$^-$	MS^2	Molecular formula (error in ppm)	Extraction solvent			References
							a	b	C	
43	18.6	Pinellic acid, trihydroxyoctadecenoic acid		329.2336	171	$C_{18}H_{34}O_5$, (0.9)	√		√	[59]
44	18.74	trihydroxyoctadecenoic acid isomer*		329.233	229, 171, 127	$C_{18}H_{34}O_5$, (0.17)	√	√	√	[68]
45	19.26	trihydroxy-octadecadienoic acid		327.2187	239, 171, 229	$C_{18}H_{32}O_5$, (0.71)	√	√	√	[59]

Solvent **a**: H_2O extract, **b**: acidified H_2O extract, **c**: 70% MeOH: H_2O.
*Compounds reported for the first time in beet leaves.
**Compounds not previously described in nature.

With the aid of feature-based molecular networking (GNPS 2) platform, isomers could be discriminated by their retention time difference within the same cluster reflecting its advantage over the classical one. Apigenin 6,8-di-*C*-hexoside isomers, compounds **17** & **18** were observed as two separate connected nodes with the same parent ion within cluster **A** in both networks (Figs. 2 & 3) indicating a possible isomeric structural features. The extracted ion chromatograms furthermore confirmed the presence of two isomers rendered as two discrete peaks eluted at 9.04 and 9.12 min. with a molecular ions [M-H]$^-$ at *m/z* 593.1515 and 595.1595 [M + H]$^+$ corresponding to a formula of $C_{27}H_{30}O_{15}$. The direct attachment of **17** & **18** to compound **10** with a mass shift of 30 Da as probable OCH_2 extension with characteristic fragments at *m/z* 473 [M-H-120]$^-$ for the cross ring cleavage of *C*-hexoside moiety and *m/z* 413 (loss of an additional 60 Da) perceived the replacement of *O*-pentoside into *C*-hexoside. Thus, both compounds were assigned as apigenin 6,8-di-*C*-glucoside, previously identified in *B. vulgaris* leaves [53]. Equivalently, two additional isomers **19** and **20** eluted at 9.30 and 9.41 min. could be recognized as two nodes linked by a thick edge with a null mass difference in the ions constellation (Fig. 2). Their linkage by delta mass of 14 (+CH_2), and 16 (-*O*) Da to **10**, and **17** & **18**, respectively propagated their assignment as apigenin *C*-deoxyhexoside-*O*-hexoside isomers boosted by MS^2 fragments at *m/z* 415 [M-H-162]$^-$ for the loss of *O*-hexose moiety and a base peak at *m/z* 311 [M-162-104-H]$^-$ indicative of *C*-deoxyhexoside moiety [52].

Within the same cluster (Fig. 2), compounds **19** & **20** were closely associated to an ion feature **21** with a mass difference of 14 Da having a parent ion at *m/z* 563.1409 [M-H]$^-$ and a formula of $C_{26}H_{28}O_{14}$. Considering the suggested MFs difference, 14 Da could point to CH_2 that was traced up in the MSMS comparatively against **19** & **20** to allocate the structural variation. A dual modification was suggested in the attached sugars as *O*-pentoside rather than *O*-hexoside concerning the fragment observed at *m/z* 413 [M-H-150]$^-$ and *C*- hexoside unit instead of *C*-deoxyhexoside corresponding to *m/z* 293 for an extra loss of 120 amu. Accordingly, it was annotated as (iso)vitexin 2″-*O*-pentoside as previously reported in beet leaves [54].

In parallel, compounds **22** and **29**, tentatively identified as (iso) vitexin-6″-malonyl-2″-*O*- pentoside, were directly recognized as likely isomeric structures since they were visualized as two bound ions sharing the same precursor ion in the same cluster within the positive network (Fig. 3). They exhibited molecular ion peaks at *m/z* 649.1415 [M-H]$^-$, 651.1561[M + H]$^+$ suggesting a molecular formula of $C_{29}H_{30}O_{17}$. Their annotation was based on their observed negative MS^2 spectra having fragment ions at *m/z* 563 [M-H-86]$^-$ accounting for the loss of a malonyl group, *m/z* 455 [M-H-44-150]$^-$ for an extra loss of 2″-*O*-pentoside moiety and the characteristic fragment at *m/z* 311 of apigenin *C*-hexosides [46].

While compound **24** appeared as a significant ion, in cluster **A** in the positive network (Fig. 3) due to its linkage to most of the constituting nodes. It was connected to compounds **10** with a mass difference of 132 Da, 162 Da to **17** & **18**, 146 Da to **19** & **20** and 86 Da to **35**. Consequently, it was assigned as apigenin *C*-hexoside possessing a parent ion at *m/z* at 433.1139 [M + H]$^+$ and 431.1056 [M-H]$^-$ and a molecular formula of $C_{21}H_{20}O_{10}$. The observation of *m/z* 343 [M + H-90]$^+$ and 313 [M + H-120]$^+$ as a supportive product ions in the positive mode clarified the cross-ring fissions in the *C*-hexoside moiety [22].

Whereas, compound **26** with [M-H]$^-$ at 679.1518, $C_{30}H_{32}O_{18}$ correlated to apigenin di-*C*-hexoside (**17** & **18**) with a mass difference of 86 Da signifying a probable malonylated derivative (Fig. 2). However, its negative MS^2 spectrum afforded a product ion at 455 [M-H-(162)-18]$^-$ which is characteristic of 2″-*O*-glycosyl-*C*-glycosyl derivatives rather than the *C*-glycosyl ones. Other observed ions were *m/z* 635 [M-H-44]$^-$ for CO_2 elimination, and 575 [M-H-86-18]$^-$ for the loss of malonyl group. Hence, it was identified as malonyl (iso)vitexin-2″-*O*-hexoside [52].

The negative EIC of 605 Da displayed 3 distinct peaks sharing the same elemental composition $C_{28}H_{30}O_{15}$. The first one eluted **23** at 9.6 min. followed by two isomers **27** & **33** at 10.31 and 10.64 min. However, their MS^2 spectra were quite different such that compound **23**, 605.1523[M-H]$^-$ showed the fragmentation pattern of acetylated 2″-*O*-pentosyl *C*-glycosides with fragments at *m/z* 563 [M-H-42]$^-$, *m/z* 413 for an extra loss of 150 Da significant of the cleavage of 2″-*O*-pentosyl moiety followed by the loss of 120 Da indicating a *C*-glycoside flavone [55]. And hence, it was supposed to be an acetyl 2″-*O*-pentosyl (iso)vitexin which was additionally certified by its presence in *C*-glycosidic flavones cluster of the spectral negative network being connected to the malonylated (iso)vitexin pentosides (**22** & **29**) with a 42 Da mass difference (Fig. 2). Inversely, the full mass spectra of **27** and **33** revealed di-*C*-glycosidic derivatives with identical fragment ions at *m/z* 563 [M-H-42]$^-$ corresponding to the loss of acetyl group, *m/z* 455 [(M-42-18)-90-H]$^-$ from the cross ring cleavage of *C*-glycosidic moieties and *m/z* 353, 311 characteristics for apigenin di-*C*-glycosides. Consequently, they were annotated as acetylated apigenin *C*-hexoside *C*-pentoside isomers [52].

Compound **28** was found with a molecular ion of 635.1626 [M-H]$^-$ and a formula of $C_{29}H_{32}O_{16}$. Its direct association to compound **23** in the negative spectral network (Fig. 2) with an extra 30 Da (OCH_2) along with its fragmentation pattern proposed a hexoside derivative rather than a pentoside one. This assumption was even confirmed by its fragmentation sequence with a fragment at 455 [M-H-180]$^-$ for the loss of 2″-*O*-hexosyl moiety followed by the loss of 42 Da at *m/z* 413 significant of its acetylation and finally a fragment at *m/z* 293 characteristic of apigenin *C*-hexosides. Accordingly, it was identified as (iso)vitexin 6″-acetyl 2″-*O*-hexoside [52].

Similarly, cluster **A** in the negative mode (Fig. 2) showed additional distinct isomers **32** and **36** with *m/z* 663.15611 [M-H]$^-$ correlated to the malonylated (iso)vitexin pentosides (**22** & **29**) with a mass shift of 14 Da which was followed in their MS^2 spectra to suggest the presence of a *O*-deoxyhexosyl moiety instead of pentosyl. This was again supported with the observed key fragment ions at *m/z* 545 [M-H-86-18]$^-$ due to loss of H_2O along with the malonyl

group, *m/z* 311 [M-H-146-120]$^-$ proving the loss of *O*-deoxyhexosyl moiety and cross cleavages of a *C*-hexosyl residue characteristic for 6″-*O*-deoxyhexosyl *C*-hexosyl derivatives [52]. Accordingly, they were tentatively assigned as malonyl 6″-*O*-deoxyhexosyl *C*-hexosyl apigenin congeners.

The EIC of *m/z* 607.1669 [M-H]$^-$ with a molecular formula of $C_{28}H_{32}O_{15}$, unexpectedly revealed two peaks as **35** and **38** at 11.20 and 12.06 min., respectively with quite different MSMS which was further validated by the spectral network as two discrete nodes. Compound **35** was found to group with the *C*-glycosidic flavones within negative cluster **B** (Fig. 2). Its MS^2 spectrum showed the presence of a fragment ion at *m/z* 487 for [M-H-120]$^-$ and the absence of the aglycone ion, which is typical of di-*C*-glycosyl flavones. This evidence, along with the UV–vis spectrum led to its assignment as dihydroxy monomethoxy flavone di-*C*-hexoside; acacetin di-*C*-hexoside [56]. Differently, compound **38** which was observed as a self-looped node and displayed a different fragmentation pattern in which daughter ions at *m/z* 457 [M-H-132-18]$^-$ characteristic for the cleavage of 2″-*O*-pentosyl moiety and *m/z* 337 [(M-H-150)-120]$^-$ typical for *C*-hexosyl derivatives were monitored. As a result, it was annotated as dihydroxy dimethoxy flavone *C*-hexoside 2″-*O*-pentoside [52].

Other flavone *C*-glycosides like **34** and **37** were also pictured as self-looped nodes in the negative mode while in the positive mode they were assembled within cluster **A** (Figs. 2 & 3). Such ion scattering in the negative mode could be explained in the light of the fewer generated fragments which are the key parameter for the ions assembling. Such ions assemblage in the positive mode propagated the annotation of these ions through the observed mass shifts of the connecting edges. For example, compound **34**, *m/z* 517.0986 [M-H]$^-$ $C_{24}H_{22}O_{13}$, was found to be in a direct connectivity with the formerly annotated apigenin *C*-hexoside **24** with a mass difference equals to 86 Da which could be possibly envisioned as an extra malonylation. The existence of confirmatory fragment ions as *m/z* 413 [M-H-86-18]$^-$ revealing the loss of a malonyl unit together with *m/z* 311 with 341 characteristics for the *C*-hexoside moiety breakdown of the flavone led to its assignment as malonyl(iso)vitexin [57].

Likewise, compound **37** was depicted as structurally related congener to **21** with an additive CH_2 taking into account the suggested molecular formulas. Manual inspection of the comparative MS^2 spectra delivered a typical fragmentation behavior to **21** with a constant mass shift of 14 Da, *m/z* 427 & 413 [M-H-150]$^-$ and *m/z* 307 & 293 [(M-H-150)-120]$^-$ permitting the allocation of such extra 14 Da on the aglycone moiety which led to its identification as acacetin *C*-hexoside-2″-*O*-pentoside [56].

A unique feature **39** appeared as a self-looped node in the negative network (Fig. 2) at *m/z* 815.2035 [M-H]$^-$ having a chemical formula $C_{38}H_{40}O_{20}$. The MS^2 spectrum showed fragment ions at *m/z* 639 [M-H-177]$^-$ pointing to a potential loss of a feruloyl moiety and *m/z* 315 [(M-H-177)-324]$^-$ for the loss of di-*O*-hexoside units (Fragmentation scheme and MS^2 spectrum are shown as **Suppl. Fig. S2, S3**). Thus, it was tentatively identified as tetrahydroxy monomethoxy flavone-*O*-feruloyl hexosyl hexoside as a possible new natural product.

While the positive spectral network (Fig. 3) revealed an ion feature **40** with a parent ion at *m/z* 665.1723 [M + H]$^+$. It was directly linked to a previously annotated acacetin *O*-pentosyl *C*-hexoside **37** and with close relatedness to compound **22** in the positive molecular network, (iso) vitexin 2″-*O*-(6″-malonyl) hexoside with a mass difference of 14 Da (CH_2) proving the methylation of the aglycone moiety. When considering the generated molecular formula of $C_{30}H_{32}O_{17}$ along with the recognized mass difference of 86 Da, a probable malonylation of **37** was assumed. Comparing the fragmentation patterns of the two compounds additionally validated this assumption where shared fragment ions from the cleavage of an *O*-pentosyl moieties [M + H-132]$^+$ at *m/z* 447 and 533 for **37** & **40,** respectively were found (Fragmentation scheme and MS^2 spectrum for compound **40** are shown as **Suppl. Fig. S4, S5**). Whereas, *m/z* 447 [M + H-132–89]$^+$ was spotted later for compound **40** from the sequential loss of a malonyl group. Other shared characteristic fragments at *m/z* 327 representing the loss of 120 Da as a cross ring cleavage of a *C*-hexoside moiety conclusively facilitated its tentative assignment as acacetin *O*-pentosyl malonyl *C*-hexoside that was not previously reported in nature.

Among the identified known *C*-glycosidic flavones: apigenin *C*-deoxyhexoside-*O*-hexoside **19** & **20**; (iso)vitexin 2″-*O*-(6″-malonyl) hexoside **22** & **33**, acetyl apigenin *C*-pentoside *C*-hexoside **27 & 32**, malonyl 6″*O*-deoxyhexosyl-*C*-hexosyl apigenin **31 & 36**, malonyl (iso)vitexin **34**, acacetin di-*C*-hexoside **35**, acacetin *C*-hexoside - 2″-*O*-pentoside **37** and dihydroxy dimethoxy flavone *C*-hexoside 2″-*O*-pentoside **38** are reported for the first time to occur in beet leaves along with the putatively annotated new compounds tetrahydroxy monomethoxy flavone-*O*-feruloyl hexosyl hexoside **39,** and acacetin *O*-pentosyl *C*-malonyl hexoside **40**.

Flavonol O-glycosides as a distinct compound family were laid out as cluster **C** having 3 closely related nodes in the negative spectral network, exclusively (Fig. 2). The first of which was isorhamnetin di-*O*- hexoside **25**, exhibited a molecular ion at *m/z* 641.172 [M + H]$^+$ and 639.1565 [M−H]$^-$ corresponding to a chemical formula of $C_{28}H_{32}O_{17}$ and fragment ions at *m/z* 317 [M + H-324]$^+$, 315 [M-H-324]$^-$ attributed to the loss of two hexose moieties [46]. Two positional diglycosylated isorhamnetin isomers **30** & **31**, *m/z* 609.1465 [M-H]$^-$, were in a direct connection to **25** with a 30 Da difference (OCH_2) proposing the replacement of one of the hexoses with a pentose moiety. This was further affirmed with the detected formula of $C_{27}H_{30}O_{16}$ and their MS^2 spectra which showed an abundant ion at *m/z* 315 [M-H-132-162]$^-$ from the loss of *O*-pentosyl and *O*-hexosyl moieties. Hence, they were tentatively assigned as not previously reported isorhamnetin *O*-pentoside *O*-hexoside isomers in beet leaves [58].

Fatty acids: additionally, the ESI-MSMS spectra showed the presence of polyhydroxylated fatty acids in the negative spectral network as an individual family (Fig. 2). The observed four nodes cluster represented two trihydroxy-octadecadienoic acid isomers **42** & **45** along with two trihydroxy-octadecenoic acid isomers **43** & **44**. They exhibited molecular ions at *m/z* 327.2178 [M−H]$^-$ ($C_{18}H_{32}O_5$) and *m/z* 329.2336 ($C_{18}H_{34}O_5$), respectively [59] with MS^2 spectra, in which sequential elimination of H_2O [M−H−18]$^-$ followed by multiple losses of CH_2 [M−H−14]$^-$ were spotted.

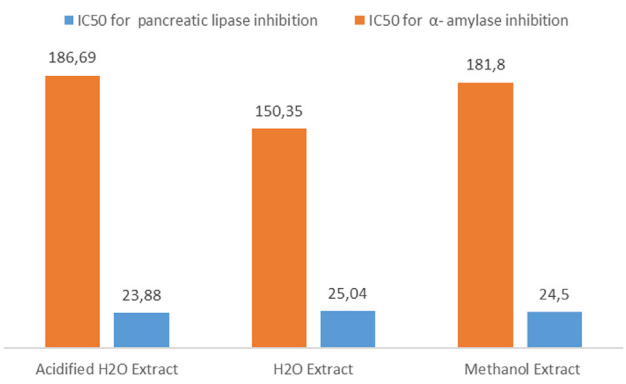

Fig. 4. IC_{50} values for the inhibition of pancreatic α- amylase and lipase enzymes with beet leaves extracts. Data are presented as (Mean ± S.D.) *: indicates significant difference at $p < 0.05$.

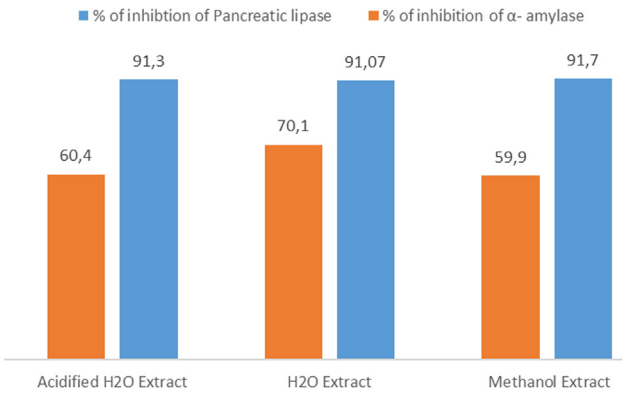

Fig. 5. Pancreatic α- amylase and lipase inhibition of beet leaves extracts at 300 ug/ml and 100 ug/ml, respectively. Data are presented as (Mean ± S.D.) *: indicates significant difference at $p < 0.05$.

Pancreatic α- amylase and lipase inhibition by different extracts of beet leaves

Lately, numerous studies have proved the potentiality of plant extracts to inhibit the digestive enzymes α-amylase and pancreatic lipase [1,34,60]. Inhibition of carbohydrate-hydrolyzing enzymes, such as α-amylase may aid in obesity management by delaying glucose absorption and overall carbohydrate digestion time. Lipase inhibition is another important tactic for obesity prevention through the suppression of triglycerides absorption.

As shown in Figs. 4 & 5, the three extracts inhibited the α-amylase activity with the lowest IC_{50} for the aqueous extract 150.35 ± 3.7 μg/ml while the other two extracts exhibited quite similar IC_{50} values. Likewise, the three extracts inhibited the pancreatic lipase equivalently as proved with their IC_{50} values with an average of 24.47 μg/ml. No significant difference was observed between the three extraction solvents regarding the percentage of the enzyme inhibition. This can be capitalized that all three designed extraction schemes are efficient enough for grabbing the active compounds to exert the desirable biological potency.

(Dose-response curves for the enzymes' activity are displayed as **Suppl. Fig. S6 & S7**. While the dose–response curve of the enzymes' inhibition with the three extracts are provided as **Suppl. Fig. S8-S13**).

The observed results could be ascribed to the phenolic metabolite(s) present in the beet leaves. Naturally occurring phenolics are reported to regulate carbohydrate and lipid metabolism, by modifying the activity of digestive enzymes [61,62]. More specifically, several investigations proved the potential health benefits of natural flavonoids in obesity management [63] especially the *C*- glycosidic flavones which exerted potent inhibitory action on pancreatic lipase as previously reported by [64]. More particular, vitexin or extracts containing vitexin were proved to exert anti-obesity activity through different mechanisms of action [65,66].

To the best of our knowledge, this is the first report for the beneficial effect of beet leaves for the prevention and/or treatment of obesity. Although the *in vivo* antidiabetic and lipid-lowering potential of beet leaves extracts were previously proved by [22,67].

Conclusion

The effectiveness of three extracting systems (H_2O, 1% acidified H_2O with ascorbic acid and 70%MeOH) of beet leaves for pulling out the secondary metabolites from the beet leaves were compared *via* holistic UPLC-HRMS/MS analysis. Molecular networking propagated metabolite profiling allowed the dereplication of 45 metabolites belonging to diverse classes among which 24 were not formerly described in beet leaves including a putative description of 2 new metabolites, namely a flavone feruloyl derivative (**39**) and a malonylated acacetin di-glycoside (**40**). Full structural elucidation of these novel metabolites using other spectroscopic techniques *i.e.,* NMR post isolation should now follows. Simultaneously, the inhibitory activities of the three extracts were tested against pancreatic α-amylase and lipase enzymes for its possible use for obesity management. All three extracting solvents were proved statistically efficient and maintained the desired biological activity. These results may help to expand the potential health benefits of beet leaves for obese people as well as being a rich source of nutraceuticals. However, additional studies are essential to determine its biological activity in more complex systems and various food matrices both in *in vitro* and *in vivo* digestion processes.

Compliance with ethics requirements

This article does not contain any studies with human or animal subjects

Declaration of Competing Interest

The authors declare that they have no known competing financial interests or personal relationships that could have appeared to influence the work reported in this paper.

Appendix A. Supplementary data

Supplementary data to this article can be found online at https://doi.org/10.1016/j.jare.2020.06.001.

References

[1] Birari RB, Bhutani KK. Pancreatic lipase inhibitors from natural sources: unexplored potential. Drug Discovery Today 2007;12(19–20):879–89.
[2] Organistaion, W.H. https://www.who.int/news-room/fact-sheets/detail/obesity-and-overweight 2016.
[3] Kakkar AK, Dahiya N. Drug treatment of obesity: current status and future prospects. European Journal of Internal Medicine 2015;26(2):89–94.
[4] Drew BS, Dixon AF, Dixon JB. Obesity management: update on orlistat. Vascular health and risk management 2007;3(6):817.
[5] Tziomalos K, Krassas GE, Tzotzas T. The use of sibutramine in the management of obesity and related disorders: an update. Vascular health and risk management 2009;5:441.
[6] de Simone G, D'Addeo G. Sibutramine: balancing weight loss benefit and possible cardiovascular risk. Nutrition, Metabolism and Cardiovascular Diseases 2008;18(5):337–41.
[7] Karamadoukis L et al. An unusual complication of treatment with orlistat. Clin Nephrol 2009;71(4):430–2.
[8] Slovacek L, Pavlik V, Slovackova B. The effect of sibutramine therapy on occurrence of depression symptoms among obese patients. Nutrition, Metabolism and Cardiovascular Diseases 2008;18(8):e43–4.
[9] Yun JW. Possible anti-obesity therapeutics from nature–A review. phytochemistry, 2010,;71(14–15):1625–41.
[10] Worsztynowicz P et al. Pancreatic α-amylase and lipase inhibitory activity of polyphenolic compounds present in the extract of black chokeberry (Aronia melanocarpa L.). Process Biochem 2014;49(9):1457–63.
[11] Andrew C. The encyclopedia of medicinal plants. A Dorling Kindersley Book; 1996.
[12] Tardío J et al. *Ethnobotanical and food composition monographs of selected Mediterranean wild edible plants*, in *Mediterranean Wild Edible*. Plants. 2016; Springer:273–470.
[13] Septembre-Malaterre A, Remize F, Poucheret P. Fruits and vegetables, as a source of nutritional compounds and phytochemicals: Changes in bioactive compounds during lactic fermentation. Food Res Int 2018;104:86–99.
[14] Nikan M, Manayi A. *Beta vulgaris L*, in *Nonvitamin and Nonmineral Nutritional*. Supplements. 2019;Elsevier:153–8.
[15] Sacan O, Yanardag R. *Antioxidant and antiacetylcholinesterase activities of chard (Beta vulgaris L. var. cicla).* Food and chemical toxicology 2010;48(5):1275–80.
[16] Ninfali P, Angelino D. Nutritional and functional potential of Beta vulgaris cicla and rubra. Fitoterapia 2013;89:188–99.
[17] Clifford T et al. The potential benefits of red beetroot supplementation in health and disease. Nutrients 2015;7(4):2801–22.

[18] Vulić JJ et al. In vivo and in vitro antioxidant effects of beetroot pomace extracts. J Funct Foods 2014;6:168–75.
[19] Jha R, Gupta RK. Development of energy drink containing Aegle marmelos, Rubia cordifolia, Phyllanthus emblica and Beta vulgaris and its phytochemical, nutritive and antimicrobial analysis. Journal of Pharmacognosy and Phytochemistry 2016;5(1):186–93.
[20] Martinez RM et al. Anti-inflammatory activity of betalain-rich dye of Beta vulgaris: effect on edema, leukocyte recruitment, superoxide anion and cytokine production. Arch Pharmacal Res 2015;38(4):494–504.
[21] Zielińska-Przyjemska M et al. In vitro effects of beetroot juice and chips on oxidative metabolism and apoptosis in neutrophils from obese individuals. Phytotherapy Research: An International Journal Devoted to Pharmacological and Toxicological Evaluation of Natural Product Derivatives 2009;23 (1):49–55.
[22] El-Ghffar EAA et al. HPLC-ESI-MS/MS analysis of beet (Beta vulgaris) leaves and its beneficial properties in type 1 diabetic rats. Biomed Pharmacother 2019;120:109541.
[23] Ben Haj Koubaier, H., et al., Betalain and phenolic compositions, antioxidant activity of Tunisian red beet (Beta vulgaris L. conditiva) roots and stems extracts. International journal of food properties, 2014. 17(9): p. 1934-1945.
[24] Nowacki L et al. Betanin-enriched Red beetroot (Beta vulgaris L.) extract induces apoptosis and autophagic cell death in MCF-7 cells. Phytother Res 2015;29(12):1964–73.
[25] Kujala T, Loponen J, Pihlaja K. Betalains and phenolics in red beetroot (Beta vulgaris) peel extracts: extraction and characterisation. Zeitschrift für Naturforschung C 2001;56(5–6):343–8.
[26] Attia GY, Moussa M, Sheashea E. *Characterization of red pigments extracted from red beet (Beta vulgaris L.) and its potential uses as antioxidant and natural food colorants.* Egyptian. Journal of Agricultural Research 2013;91(3):1095–110.
[27] Azizah AN et al. The Use of Natural Dyes from Beetroot Skin Extract (Beta Vulgaris) as Teaching Material on Cell Division for Senior High School Students. Indonesian Journal on Learning and Advanced Education (IJOLAE) 2019;2(1):20–6.
[28] Garg N et al. Mass spectral similarity for untargeted metabolomics data analysis of complex mixtures. Int J Mass Spectrom 2015;377:719–27.
[29] Olmo-García L et al. Exploring the Capability of LC-MS and GC-MS Multi-Class Methods to Discriminate Virgin Olive Oils from Different Geographical Indications and to Identify Potential Origin Markers. Eur J Lipid Sci Technol 2019;121(3):1800336.
[30] Dührkop K et al. Searching molecular structure databases with tandem mass spectra using CSI: FingerID. Proc Natl Acad Sci 2015;112(41):12580–5.
[31] Böcker S, Dührkop K. *Fragmentation trees reloaded.* Journal of cheminformatics 2016;8(1):5.
[32] Zani CL, Carroll AR. Database for rapid dereplication of known natural products using data from MS and fast NMR experiments. J Nat Prod 2017;80 (6):1758–66.
[33] Miller GL. Use of dinitrosalicylic acid reagent for determination of reducing sugar. Anal Chem 1959;31(3):426–8.
[34] Marrelli M et al. Inhibition of key enzymes linked to obesity by preparations from Mediterranean dietary plants: effects on α-amylase and pancreatic lipase activities. Plant Foods Hum Nutr 2013;68(4):340–6.
[35] Conforti F et al. Wild Mediterranean dietary plants as inhibitors of pancreatic lipase. Phytother Res 2012;26(4):600–4.
[36] Uysal S et al. A comparative in vitro and in silico study of the biological potential and chemical fingerprints of Dorcycinum pentapyllum subsp. haussknechtii using three extraction procedures. New J Chem 2017;41 (22):13952–60.
[37] Chiocchio I et al. Screening of a hundred plant extracts as tyrosinase and elastase inhibitors, two enzymatic targets of cosmetic interest. Ind Crops Prod 2018;122:498–505.
[38] Wang M et al. Sharing and community curation of mass spectrometry data with Global Natural Products Social Molecular Networking. Nat Biotechnol 2016;34(8):828.
[39] Stintzing FC, Schieber A, Carle R. Identification of betalains from yellow beet (Beta vulgaris L.) and cactus pear [Opuntia ficus-indica (L.) Mill.] by high-performance liquid chromatography– electrospray ionization mass spectrometry. J Agric Food Chem 2002;50(8):2302–7.
[40] Diem S, Bergmann J, Herderich M. Tryptophan-N-glucoside in fruits and fruit juices. J Agric Food Chem 2000;48(10):4913–7.
[41] Liu S et al. Characterization of compounds and potential neuraminidase inhibitors from the n-butanol extract of Compound Indigowoad Root Granule using ultrafiltration and liquid chromatography–tandem mass spectrometry. J Pharm Biomed Anal 2012;59:96–101.
[42] Lan MS et al. Chemical constituents of Phyllanthus reticulatus. Helv Chim Acta 2010;93(11):2276–80.
[43] Hama JR, Strobel BW. Pyrrolizidine alkaloids quantified in soil and water using UPLC-MS/MS. RSC Adv 2019;9(52):30350–7.
[44] Peng H et al. Major chemical constituents and antioxidant activities of different extracts from the peduncles of Hovenia acerba Lindl. Int J Food Prop 2018;21(1):2135–55.
[45] Pan Z et al. Non-targeted metabolomic analysis of orange (Citrus sinensis [L.] Osbeck) wild type and bud mutant fruits by direct analysis in real-time and HPLC-electrospray mass spectrometry. Metabolomics 2014;10(3):508–23.
[46] Vissers A et al. Enzymatic browning in sugar beet leaves (Beta vulgaris L.): influence of caffeic acid derivatives, oxidative coupling, and coupled oxidation. J Agric Food Chem 2017;65(24):4911–20.
[47] Guan H et al. Identification of the Chemical Constituents of an Anti-Arthritic Chinese Medicine Wen Luo Yin by Liquid Chromatography Coupled with Mass Spectrometry. Molecules 2019;24(2):233.
[48] Garcez WS, Yoshida M, Gottlieb OR. Benzylisoquinoline alkaloids and flavonols from Ocotea vellosiana. Phytochemistry 1995;39(4):815–6.
[49] Chin Y-W et al. Two new phenylpropanoid glycosides from the aerial parts of Paederia scandens. Bull Korean Chem Soc 2010;31(4):1070–2.
[50] Bokern M et al. Ferulic acid conjugates and betacyanins from cell cultures of Beta vulgaris. Phytochemistry 1991;30(10):3261–5.
[51] Song Q et al. Potential of hyphenated ultra-high performance liquid chromatography-scheduled multiple reaction monitoring algorithm for large-scale quantitative analysis of traditional Chinese medicines. RSC Adv 2015;5(71):57372–82.
[52] Farag MA et al. Comparative metabolite profiling and fingerprinting of genus Passiflora leaves using a multiplex approach of UPLC-MS and NMR analyzed by chemometric tools. Anal Bioanal Chem 2016;408(12):3125–43.
[53] Simirgiotis M et al. The Passiflora tripartita (Banana Passion) fruit: A source of bioactive flavonoid C-glycosides isolated by HSCCC and characterized by HPLC–DAD–ESI/MS/MS. Molecules 2013;18(2):1672–92.
[54] Ninfali P et al. Characterization and biological activity of the main flavonoids from Swiss Chard (Beta vulgaris subspecies cycla). Phytomedicine 2007;14(2–3):216–21.
[55] Zheleva-Dimitrova D et al. Chemical characterization with in vitro biological activities of Gypsophila species. J Pharm Biomed Anal 2018;155:56–69.
[56] Barreca D et al. Kumquat (Fortunella japonica Swingle) juice: Flavonoid distribution and antioxidant properties. Food Res Int 2011;44(7):2190–7.
[57] Alamgir KM et al. Acylflavonoid C-glycosides from Eleusine coracana. Phytochem Lett 2008;1(2):111–4.
[58] Wang D-M et al. A new isorhamnetin glycoside and other phenolic compounds from Callianthemum taipaicum. Molecules 2012;17(4):4595–603.
[59] Hamberg M, Olsson U. Efficient and Specific Conversion of 9-Lipoxygenase Hydroperoxides in the Beetroot. *Formation of Pinellic Acid.* Lipids 2011;46 (9):873–8.
[60] Dastjerdi ZM, Namjoyan F, Azemi ME. Alpha amylase inhibition activity of some plants extract of Teucrium species. European Journal of Biological Sciences 2015;7(1):26–31.
[61] Ikarashi N et al. The inhibition of lipase and glucosidase activities by acacia polyphenol. Evidence-Based Complementary and Alternative Medicine 2011;2011.
[62] Tadera K et al. Inhibition of α-glucosidase and α-amylase by flavonoids. J Nutr Sci Vitaminol 2006;52(2):149–53.
[63] Kawser Hossain M et al. Molecular mechanisms of the anti-obesity and anti-diabetic properties of flavonoids. Int J Mol Sci 2016;17(4):569.
[64] Lee EM et al. Pancreatic lipase inhibition by C-glycosidic flavones isolated from Eremochloa ophiuroides. Molecules 2010;15(11):8251–9.
[65] Yang JH et al. Potent anti-inflammatory and antiadipogenic properties of bamboo (Sasa coreana Nakai) leaves extract and its major constituent flavonoids. J Agric Food Chem 2017;65(31):6665–73.
[66] Wang F et al. Vitexin alleviates lipopolysaccharide-induced islet cell injury by inhibiting HMGB1 release. Mol Med Rep 2017;15(3):1079–86.
[67] Al-Dosari M et al. Effect of Beta vulgaris L. on cholesterol rich diet-induced hypercholesterolemia in rats. Farmacia 2011;59:669–78.
[68] Tao Y et al. Ultrafiltration coupled with high-performance liquid chromatography and quadrupole-time-of-flight mass spectrometry for screening lipase binders from different extracts of Dendrobium officinale. Anal Bioanal Chem 2015;407(20):6081–93.